


RESEARCH ARTICLE

The effect on precision and T1 bias comparing two flip angles when estimating muscle fat infiltration using fat-referenced chemical shift-encoded imaging

Anette Karlsson^{1,2}  | Anneli Peolsson^{2,3} | Thobias Romu⁴ |
Olof Dahlqvist Leinhard^{2,4,5} | Anna-Clara Spetz Holm⁶ | Sofia Thorell⁶ |
Janne West^{1,2,4} | Magnus Borga^{1,2,4}

¹Department of Biomedical Engineering, Linköping University, Linköping, Sweden

²Center for Medical Image Sciences and Visualization (CMIV), Linköping University, Linköping, Sweden

³Department of Health, Medicine and Caring Sciences, unit of Physiotherapy, Linköping University, Linköping, Sweden

⁴AMRA Medical AB, Linköping, Sweden

⁵Department of Health, Medicine and Caring Sciences, Linköping University, Linköping, Sweden

⁶Department of Biomedical and Clinical Sciences, Faculty of Medicine and Health Sciences, Linköping University, Linköping, Sweden

Correspondence

Anette Karlsson, Medicinsk Strålningsfysik, O-huset, plan 08, Linköping University Hospital, SE-581 85 Linköping, Sweden.
Email: anette.karlsson@regionostergotland.se

Funding information

Vetenskapsrådet, Grant/Award Number: VR 2019-0475

Investigation of the effect on accuracy and precision of different parameter settings is important for quantitative MRI. The purpose of this study was to investigate T1 bias and precision for muscle fat infiltration (MFI) measurements using fat-referenced chemical shift MFI measurements at flip angles of 5° and 10°. The fat-referenced measurements were compared with fat fractions, which is a more commonly used measure of MFI. This retrospective study was performed on data from a clinical intervention study including 40 postmenopausal women. Test and retest images were acquired with a 3-T scanner using four-point 3D spoiled gradient multiecho acquisition. Postprocessing included T2* correction and fat-referenced calibration, where the fat signal was calibrated using adipose tissue as reference. The mean MFI was calculated in six different muscle regions using both the fat-referenced fat signal and the fat fraction, defined as the fat signal divided by the sum of the fat and water signals. Both methods used the same fat and water images as input. The variance of the difference between mean MFI from test and retest was used as the measure of precision. The signal-to-noise ratio (SNR) characteristics were analyzed by measuring the full width at half maximum (FWHM) of the fat signal distribution. There was no difference in the mean MFI at different flip angles for the fat-referenced technique ($p = 0.66$), while the measured fat fractions were 3.3 percentage points larger for 10° compared with 5° ($p < 0.001$). No significant difference in the precision was found in any of the muscles analyzed. However, the FWHM of the fat signal distribution was significantly ($p = 0.01$) lower at 10°. This strengthens the hypothesis that fat-referenced MFI is insensitive to flip angle-induced T1 bias in CSE-MRI, enabling usage of a higher and more SNR-effective flip angle. The lower FWHM in fat-referenced MFI at 10° indicates that high flip angle acquisition is advantageous even although no significant differences in precision were observed comparing 5° and 10°.

Abbreviations used: CLIC, consistent intensity inhomogeneity correction; FF, fat fraction; FWHM, full width at half maximum; MFI, muscle fat infiltration; PDF, proton density fat fraction; SD, standard deviation; Sw, within-subject standard deviation; wCV, within-subject coefficient of variation.

This is an open access article under the terms of the Creative Commons Attribution-NonCommercial-NoDerivs License, which permits use and distribution in any medium, provided the original work is properly cited, the use is non-commercial and no modifications or adaptations are made.

© 2021 The Authors. *NMR in Biomedicine* published by John Wiley & Sons Ltd.

KEYWORDS

chemical shift-encoded MRI, flip angle, magnetic resonance imaging, muscle fat infiltration, quantification

1 | INTRODUCTION

Muscle fat infiltration (MFI) has been related to several health conditions such as functional outcomes in sarcopenia,¹ chronic pain,^{2–4} inflammation,⁵ muscular dystrophy^{6,7} and type II diabetes.⁸ To correctly diagnose, monitor and investigate intervention progression of MFI in these diseases or syndromes, high accuracy and precision are needed. Challenges with MFI estimation include large variations both between muscles⁹ and within the same muscle,^{10,11} as well as the need for quantifying fat fractions (FFs) as low as 0.5%.¹² Without high precision in the measurements, the aforementioned challenges make it very difficult to detect and quantify intervention effects.

Magnetic resonance imaging (MRI) enables noninvasive, high soft tissue contrast images with the possibility of 3D volume acquisition. High soft tissue contrast and volumetric image acquisition are important for quantification of low FFs and for the ability to distinguish different muscles from each other. Furthermore, accurate quantification of fat infiltration is possible using chemical shift MRI, if confounding factors, such as T2* relaxation, compensation for multiple lipid peaks and T1-weighting bias are taken into consideration and possibly corrected for.^{13,14} The chemical shift imaging technique utilizes the different resonance frequencies of water protons and the protons of triglyceride molecules to separate the water signal from the fat signal.¹⁵

A well-established measurement for MRI-based fat quantification is proton density fat fraction (PDFF), often calculated as the ratio between the fat signal and the total fat and water signal corrected for the aforementioned confounding factors.¹⁶ A common approach to mitigate the T1-weighting bias is to use a low flip angle (1–3° at 3 T) together with a sufficiently long repetition time (TR). However, the low flip angle required to avoid T1 bias also lowers the signal-to-noise ratio (SNR). High SNR is crucial when the measured signal is expected to be low. For example, Hong et al. showed that the reconstruction of noise leads to a false detection of fat within the spleen, an organ normally without fat deposition.¹⁷ The T1 bias can also be corrected for using literature values of the T1-relaxation times for the water and fat signal.¹⁸

Another approach to quantify FF is with fat-referenced chemical shift imaging.^{19,20} After automatic detection of voxels with pure adipose tissue within the image followed by a calibration of the fat image using the detected adipose tissue as reference (fat/fat^{ref}), the fat images contain quantitative information.²¹ Subsequently, the PDFF can be obtained for each voxel, enabling MFI calculation without information from the water signal and therefore theoretically invariant to T1 bias. This invariance to T1 bias has also been shown in a small study performed by Peterson et al.²² SNR can therefore be increased by increasing the flip angle, potentially improving the precision, without decreasing the accuracy of the FF estimate.

The study by Peterson et al. also reported an increased precision comparing a high flip angle with a low flip angle using the fat-referenced technique.²² However, the analysis was based only on the standard deviation (SD) in a limited region of interest in a few 2D slices, leading to high sensitivity to anatomical variation. To distinguish anatomical variation from signal measurement precision, whole-muscle coverage would be needed.

In the current study we wanted to distinguish signal measurement precision from potential segmentation errors due to noisy images in the whole-muscle coverage segmentation. Because the fat-referenced method for MFI estimation is T1-invariant, higher flexibility regarding the choice of flip angle, without increased scan time, is possible. In this study, two flip angles, 5° and 10°, were chosen. A study by Kühn et al. showed that 10° gave the highest SNR when comparing flip angles of 1, 3, 5, 10 and 20°,¹⁸ but also that a 5° flip angle has sufficient SNR to avoid segmentation errors.

The aim of the current study was therefore to compare FF with fat-referenced MFI using acquisitions with 5° and 10° flip angles to investigate differences in precision with 3D whole muscle volume coverage.

2 | EXPERIMENTAL

2.1 | Participants

Forty postmenopausal women were included in this study. The mean age \pm SD was 56 ± 6 years, ranging from 45 to 70 years. The mean body mass index (BMI) was 26.9 ± 4.0 kg/m², ranging from 19.0 to 39.0 kg/m². The participants were included from an ongoing randomized controlled trial (RCT) study (NCT01987778). One objective of the RCT was to investigate potential changes in body composition after a resistance training intervention.²³ All participants in the RCT who volunteered for an MRI scan were also included in the current study at baseline. The

RCT study was approved by The Regional Ethical Review Board in Linköping, Sweden (no: 2013/285–31), and all participants provided written informed consent prior to participating in this study. The study was performed according to the Declaration of Helsinki and Good Clinical Practice.

Inclusion criteria for participating in the RCT were postmenopausal women aged 45 years or older with low physical activity. A full description of the inclusion/exclusion criteria for the main RCT is reported in Berin et al.²³

2.2 | Data acquisition

MR images were acquired using a Philips Ingenia 3.0-T scanner (Philips, Best, The Netherlands). Each participant was scanned twice on one occasion. First, two whole-body datasets were acquired using the flip angles 5° and 10°. All other parameter settings were kept constant. After the first acquisitions, participants were repositioned (i.e. left the scanner room) and the scanning protocol was repeated. In total, four whole-body datasets were acquired for each participant.

The protocol used a four-point 3D spoiled gradient multiecho acquisition including real and imaginary images for reconstruction. Two total head-foot coverage (1.76 m) images were acquired using 10 × two (alternating the flip angle) slabs of axial images with a 25-m overlap. The nonbreath-hold slabs (1 and 7–10) consisted of 66 slices. The breath-hold sequences (2–6) consisted of 39 slices accelerated using a SENSE factor of 1.6. Each breath hold was 17 s, acquired after expiration. The repetition time (TR) was 6.69 ms, the echo times (TEs) were 1.15/2.30/3.45/4.60 ms, and the voxel size was 2.5 × 2.5 × 4 mm³ for all slabs. The total acquisition time for each scan was 8 min.

2.3 | Quantification of MFI

Water and fat images were reconstructed using phase-sensitive reconstruction²⁴ with a six-peak lipid model¹³ including T2* correction.¹⁴ Calibration of the images into fat-referenced images was performed using consistent intensity inhomogeneity correction (CIIC).²¹ Briefly, the technique calibrates the signal by normalizing the local fat signal using spatially close pure fat tissue voxels. Pure adipose tissue voxels are set to the value 1 and the rest of the image voxels are calibrated, resulting in voxels with information regarding the relative fat content compared with pure adipose tissue. This calibration produces a quantitative fat image, removing the effects of variations in signal intensity due to, for example, coils and B0-inhomogeneities.²¹ Furthermore, correction was made for the artificial amplitude slope that occurs due to the switching gradient polarities between in-phase and out-of-phase echo in the bipolar data acquisition.²⁵

The regions of interest were acquired using manually predefined labels that were registered onto the target volume.²⁶ Quality control of the automatic segmentations was performed and local adjustments were made by a blinded operator, when needed. In total, six different muscle regions were analyzed in this study: the rectus femoris, anterior thigh and posterior thigh segmented for the left and right side individually. The anterior and posterior thigh have been shown to provide excellent automatic segmentations.²⁵ Therefore, these regions were interesting to minimize the risk of segmentation errors. In addition, these muscles were also analyzed in the UK Biobank cohort,²⁷ investigating why potential bias in the measurements could be of high interest. Rectus femoris was analyzed to investigate the repeatability in a muscle that is assumed to have a low mean fat infiltration in addition to a low anatomical variance.

The left and right side of rectus femoris, anterior thigh and posterior thigh were each pooled together, resulting in three additional muscle regions. The anterior and posterior thighs were pooled together to acquire the total thigh MFI, resulting in a total of 10 muscle regions.

MFI is defined here as fat infiltration within the part of the muscle where the fat signal is less than 50%. When the muscle definition contains several muscles (e.g. left anterior thigh), removal of fat signal larger than 50% removes the contribution from intermuscular fat. Furthermore, the removal also makes MFI more robust to potential oversegmentations into subcutaneous tissue.²⁶ This MFI definition has been used in clinical studies where fat infiltration in patients with chronic pain have been studied.^{3,4} The MFI was calculated as

$$MFI [\%] = 0.937 \cdot \frac{\sum f_{RFC}(Mask(f_{RFC} < 0.5))}{\sum Mask}, \quad (1)$$

where the 0.937 is a scaling by the PDFF of adipose tissue, which is a constant that has been previously used for this purpose in a number of studies.^{9,28} *Mask* is the defined region of interest for each specific muscle region and *Fat* represents the calibrated fat signal image volume.

The FF is defined as

$$FF [\%] = \sum Fat \left(\frac{Mask(f_{RFC} < 0.5)}{\sum (f_{RFC}(Mask(f_{RFC} < 0.5)) + Water(Mask(f_{RFC} < 0.5)))} \right), \quad (2)$$

where *Water* represents the water signal image volume, calculated to evaluate the influence of T1 bias. Note that this definition requires fat-referenced signal calibration and was used to ensure the same region of interest as for fat-referenced MFI.

2.4 | Statistics

Descriptive measurements of the MFI were calculated as mean \pm SD. The within-subject standard deviation (*Sw*), that is, the SD of differences between repeated measurements on the same subject,²⁹ and limits of agreement, were calculated for fat-referenced MFI and FF at both flip angles. The within-subject coefficient of variation (*wCV*) was calculated as *Sw*/mean.

To test potential differences in precision and repeatability, the SD of the difference between test and retest was calculated and an F-test was performed between 5° and 10°. This was done with the assumption that the expected mean of the difference is zero. Therefore, a narrower SD around the mean would indicate better precision and repeatability.

Histograms over the fat-referenced MFI for all voxels in each segmentation were created to isolate the SNR effects. The full width at half maximum (FWHM) was calculated for each segmentation and a paired t-test was performed (after testing for normality using the Shapiro–Wilk test for normality) to test if there were significant differences between the flip angles. Statistical analyses were performed with R version 3.6.1 (The R Foundation).

3 | RESULTS

The reconstructions into calibrated fat and water images were successful for all participants, for both the 5° and 10° flip angles. T1 bias was visible in the in-phase images, where less contrast between the water and fat channels was present in the 5° data compared with the 10° data. In Figure 1, in-phase images are shown to illustrate the T1 bias between 5° and 10°. Furthermore, in Figure 1, calibrated fat images are shown to illustrate the nonvisible difference between 5° and 10°. More examples over a lean (BMI 19 kg/m²) and an obese subject (BMI 33 kg/m²) are illustrated in Figure S1.

The automatic segmentation of the six different muscles (bilateral segmentations of rectus femoris, anterior thigh and posterior thigh) were successful in all four images for all 40 participants. Quality assurance, including adjustments if necessary, was completed for all 960 muscle regions (40 [subjects] \times 6 [regions] \times 2 [FA] \times 2 [scans]). An example of the segmentation results can be seen in Figure 2.

The mean MFI among all participants at 5° and 10° was 5.5% and 5.2% for the rectus femoris, 7.8% and 7.7% for the anterior thigh, and 11.3% and 11.3% for the posterior thigh, respectively. No significant difference ($p = 0.66$) in MFI was observed comparing 5° and 10° flip angles in fat-referenced MRI. MFI from FF was 3.3 percentage points larger for 10° compared with 5° ($p < 0.001$). A graph showing the mean \pm SD is presented in Figure 3. In Figure 4, scatter plots over the MFI value in each voxel at flip angle 5° against 10° of the left rectus femoris for both the FF and fat-referenced method are shown. While the fat-referenced measurements approximately follow the identity line for all MFI values, those for the FF tend to overestimate all values not close to zero or one.

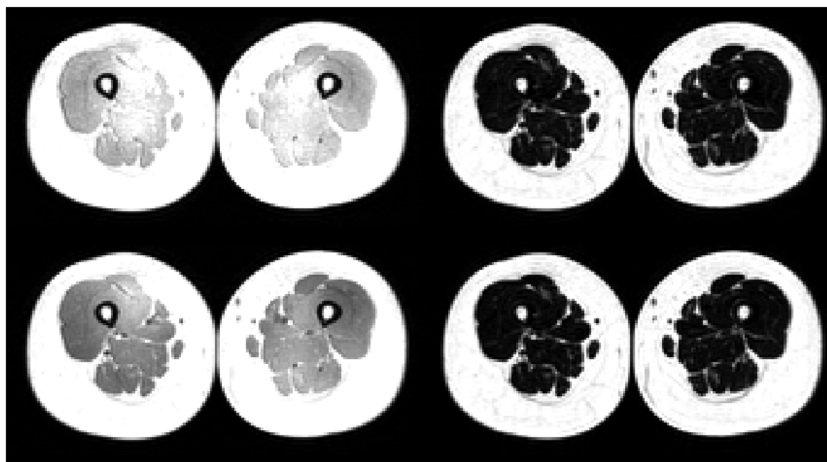


FIGURE 1 Transversal slices of the thighs of the participant closest to the mean age and body mass index (BMI) (56-year-old participant with a BMI of 27.5 kg/m²) from two scans acquired at the same time point alternating the flip angle between 5° (upper row) and 10° (lower row). The left column shows in-phase images illustrating the T1-effect between 5° and 10°. The right column shows calibrated fat images

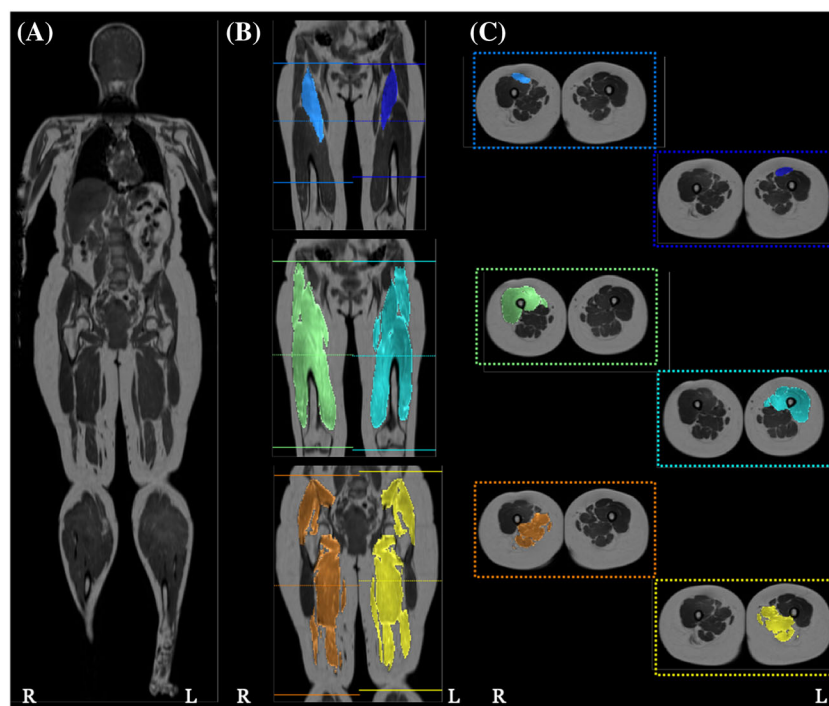


FIGURE 2 The participant closest to the mean age and body mass index (BMI) (56-year-old participant with a BMI of 27.5 kg/m²) was chosen to visualize (A) whole body coronal slice of the fat + water image, (B) coronal slice illustrating rectus femoris (top), anterior thigh (middle) and posterior thigh (bottom), and (C) the middle slice for the muscles (top to bottom) right (R) rectus femoris, left (L) rectus femoris, right anterior thigh, left anterior thigh, right posterior thigh and left posterior thigh

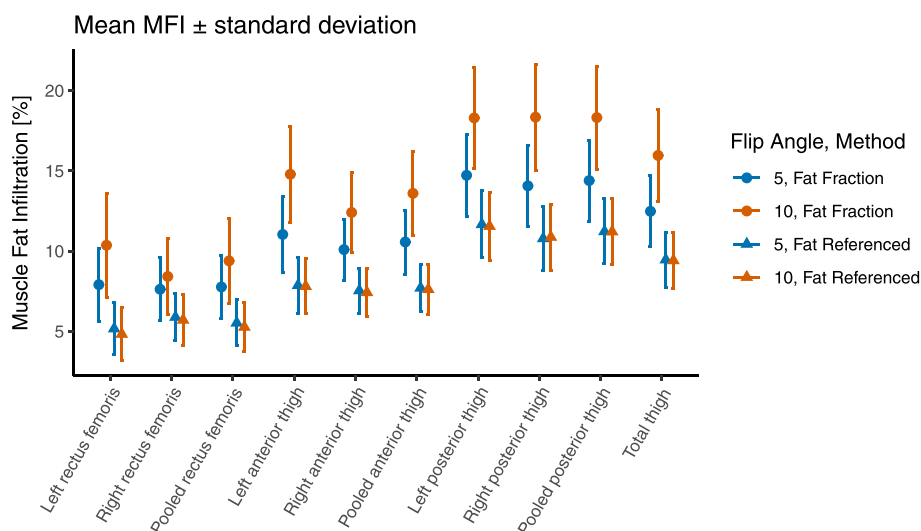


FIGURE 3 Illustration of mean \pm standard deviation of muscle fat infiltration (MFI) in the 40 participants for all 10 regions of interest (rectus femoris, anterior thigh and posterior thigh bilateral) and pooled means from left and right on the three muscles and pooled total thigh based on the anterior and posterior estimates

No differences in wCV (illustrated in Figure 5) or Sw were observed when alternating the flip angle or type of measurement (fat-referenced or FF) (Table 1). The SD of the difference between test and retest for fat-referenced MFI showed no significant differences between 5° and 10°. All SDs of the differences are presented in Table 2. The F-ratios between the four different measurements (fat-referenced and FF for whole volume and middle slice) are illustrated in Figure 6.

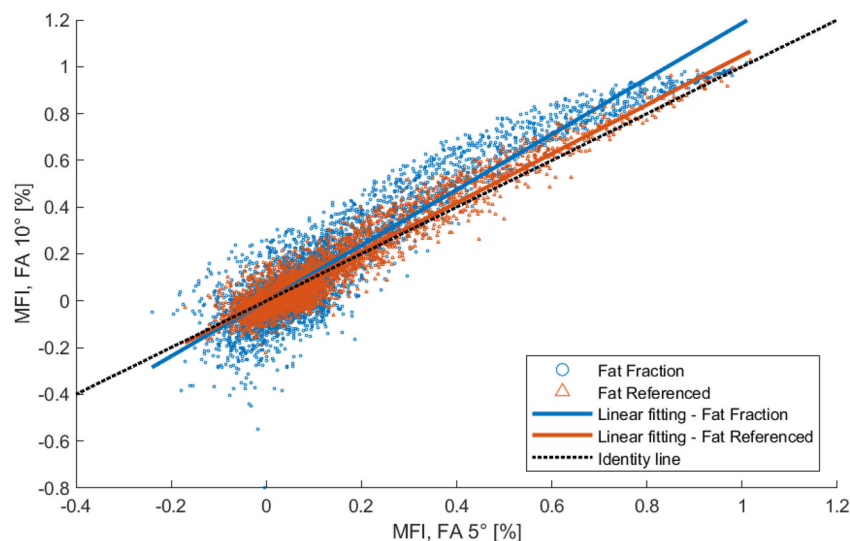


FIGURE 4 A scatter plot of the muscle fat infiltration (MFI) in each muscle of the left rectus femoris muscle in the participant closest to the mean age and body mass index (BMI) (56-year-old participant with BMI of 27.5 kg/m²). This is shown for fat fraction (blue) and fat-referenced (triangles). The identity line (dotted black line) and linear fitting of fat fraction data (blue) and fat-referenced data (triangles) are also shown

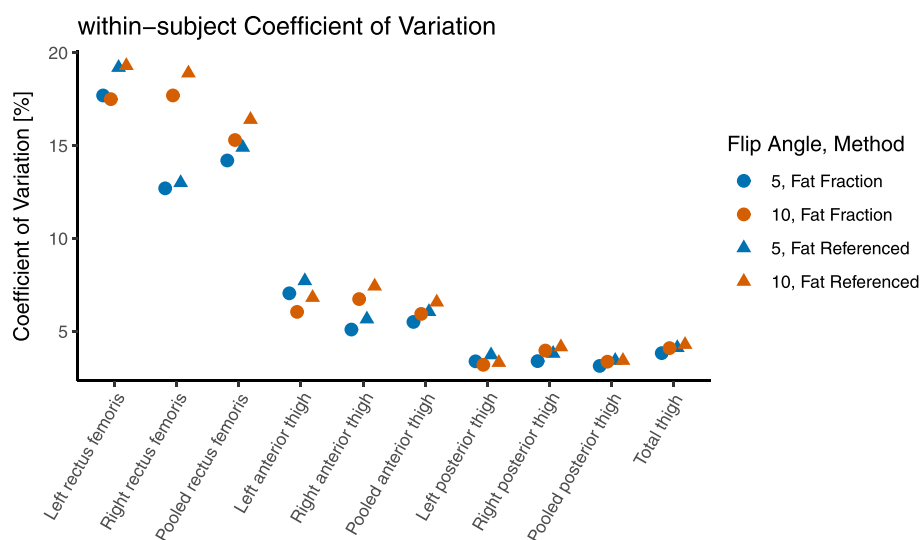


FIGURE 5 Within-subject coefficient of variation using two different flip angles (labeled with different colors) for two methods for acquiring muscle fat infiltration (MFI) (labeled with different shapes) in the 40 participants for all 10 regions of interest (rectus femoris, anterior thigh and posterior thigh bilateral) and pooled means from left and right on the three muscles and pooled total thigh based on the anterior and posterior estimates

Figure 7 shows fat-referenced MFI histograms over all voxels in the left anterior thigh. The horizontal lines show where the FWHM distances were calculated (in % units). The paired t-test between the FWHM distances (Table 3) shows that the FWHM was significantly lower at the flip angle of 10° compared with 5° in the left and pooled rectus femoris, left, right and pooled anterior thigh, and the total thigh estimate. Table 3 shows t-tests, including the resulting *p* values and 95% confidence intervals.

4 | DISCUSSION

This study showed that fat-referenced MFI measurements were not affected by T1 bias when increasing the flip angle from 5° and 10°. This is shown by Figure 3, where the mean MFI at 5° is equal to the mean MFI at 10° for all the included muscle groups. Because the T1 weighting

TABLE 1 The within-subject coefficient of variation (wCV), the within-subject standard deviation (Sw) and lower and upper limits of agreement (LoA) for the muscle fat infiltration (MFI) are shown for the 10 different muscles at 5° and 10° for fat-referenced and fat fraction

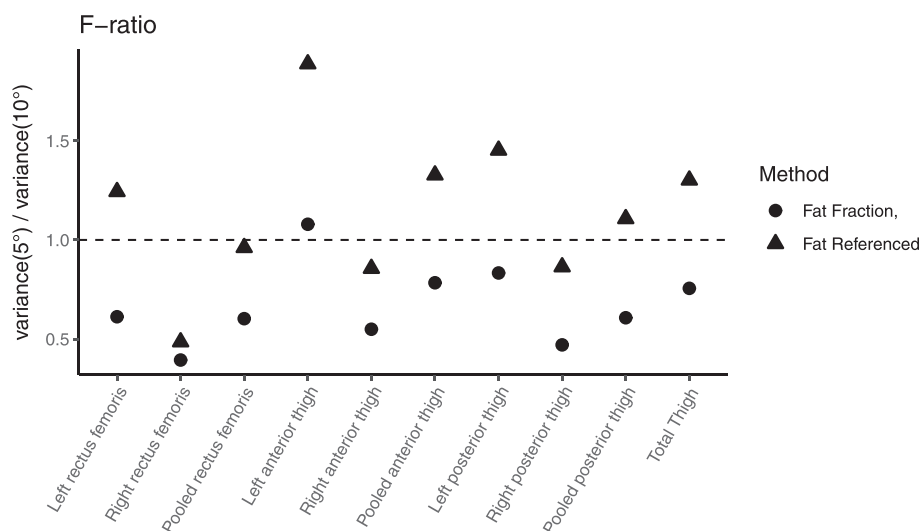
Measurand	Type	Flip angle	wCV	Sw	LoA	
Left rectus femoris (%)	Fat-referenced	5°	19.2	0.99	−2.80	2.73
		10°	19.3	0.92	−2.90	1.83
	fat fraction	5°	17.7	1.39	−3.92	3.86
		10°	17.5	1.81	−5.67	3.68
Right rectus femoris (%)	Fat-referenced	5°	13.0	0.76	−1.87	2.31
		10°	18.9	1.06	−3.28	2.45
	Fat fraction	5°	12.7	0.96	−2.34	2.93
		10°	17.7	1.47	−4.51	3.48
Pooled rectus femoris (%)	Fat-referenced	5°	14.9	0.82	−2.19	2.38
		10°	16.4	0.85	−2.68	1.73
	Fat fraction	5°	14.2	1.10	−2.94	3.20
		10°	15.3	1.42	−4.45	2.94
Left anterior thigh (%)	Fat-referenced	5°	7.72	0.61	−1.72	1.68
		10°	6.82	0.53	−1.66	0.88
	Fat fraction	5°	7.05	0.78	−2.24	2.11
		10°	6.05	0.89	−2.80	1.46
Right anterior thigh (%)	Fat-referenced	5°	5.66	0.43	−1.15	1.23
		10°	7.43	0.55	−1.71	0.83
	Fat fraction	5°	5.10	0.51	−1.42	1.47
		10°	6.74	0.83	−2.60	1.24
Pooled anterior thigh (%)	Fat-referenced	5°	6.06	0.47	−1.30	1.32
		10°	6.57	0.50	−1.55	0.71
	Fat fraction	5°	5.51	0.58	−1.65	1.61
		10°	5.94	0.80	−2.50	1.15
Left posterior thigh (%)	Fat-referenced	5°	3.73	0.43	−1.25	1.19
		10°	3.32	0.38	−1.19	0.84
	Fat fraction	5°	3.39	0.50	−1.46	1.33
		10°	3.20	0.59	−1.83	1.23
Right posterior thigh (%)	Fat-referenced	5°	3.81	0.41	−1.25	1.01
		10°	4.16	0.45	−1.40	1.01
	Fat fraction	5°	3.40	0.48	−1.45	1.16
		10°	3.97	0.73	−2.27	1.54
Pooled posterior thigh (%)	Fat-referenced	5°	3.43	0.38	−1.15	0.99
		10°	3.43	0.38	−1.20	0.83
	Fat fraction	5°	3.14	0.45	−1.36	1.14
		10°	3.37	0.62	−1.94	1.27
Total thigh (%)	Fat-referenced	5°	4.12	0.39	−1.13	1.06
		10°	4.29	0.40	−1.26	0.66
	Fat fraction	5°	3.83	0.48	−1.40	1.27
		10°	4.10	0.65	−2.04	1.04

is more prominent at 10° than 5°, a higher MFI estimate should have occurred at 10° compared with 5° if the data were affected by T1 bias in the same way as for FF techniques. Such an overestimation was seen in the FF-based MFI estimate, which is in line with the theory, because that measurement (Equation 2) is based on both the fat and water signals. In addition, the FF-based MFI was higher than the fat-referenced MFI even at 5°, which further suggests a T1-bias invariance of the fat-referenced MFI measurement, even if no true proton density-weighted data were used in this study.

TABLE 2 Standard deviation (SD) of the difference for the muscle fat infiltration (MFI) between test and retest for 5° flip angle and 10° flip angle for both fat-referenced and fat fraction values

Measurand	Type	SD (diff) 5°	SD (diff) 10°	p value
Left rectus femoris (%)	Fat-referenced	1.41	1.21	0.34
	Fat fraction	1.99	2.39	0.26
Right rectus femoris (%)	Fat-referenced	1.07	1.46	0.05
	Fat fraction	1.34	2.03	0.02
Pooled rectus femoris (%)	Fat-referenced	1.17	1.13	0.83
	Fat fraction	1.57	1.89	0.25
Left anterior thigh (%)	Fat-referenced	0.87	0.65	0.07
	Fat fraction	1.11	1.09	0.90
Right anterior thigh (%)	Fat-referenced	0.61	0.65	0.69
	Fat fraction	0.74	0.98	0.08
Pooled anterior thigh (%)	Fat-referenced	0.67	0.58	0.36
	Fat fraction	0.83	0.93	0.49
Left posterior thigh (%)	Fat-referenced	0.62	0.52	0.27
	Fat fraction	0.71	0.78	0.55
Right posterior thigh (%)	Fat-referenced	0.57	0.62	0.67
	Fat fraction	0.67	0.97	0.02
Pooled posterior thigh (%)	Fat-referenced	1.16	1.05	0.54
	Fat fraction	0.64	0.82	0.12
Total thigh (%)	Fat-referenced	0.56	0.49	0.44
	Fat fraction	0.68	0.79	0.37

Significant values (at level 0.05) are shown in bold.

**FIGURE 6** F-ratio (variance of the test–retest muscle fat infiltration [MFI] difference of 5° divided by the variance of the test–retest MFI difference of 10°) for fat-referenced MFI (triangles) and corresponding F-ratios for fat fraction MFI (circles). The dashed line represents an F-ratio of one (i.e. where the variance of 5° equals the variance of 10°)

The effect of the T1 bias when using the FF technique is highest in voxels with intermediate FFs (i.e. with partial volume effects between fat and water), which can be seen by the arc-shaped distribution of the FF measurements in Figure 4. By contrast, the fat-referenced measurements are closer to the identity line. This further indicates an insensitivity of T1 bias in the fat-referenced technique.

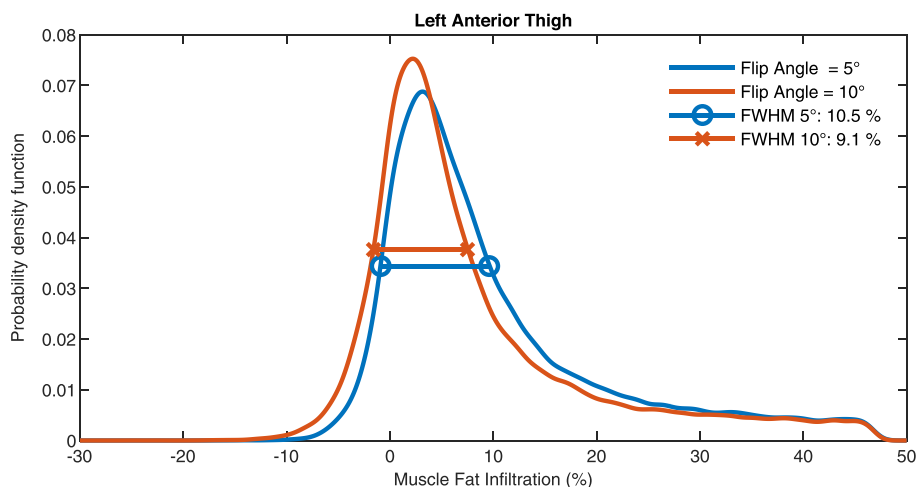


FIGURE 7 Illustration of the full width at half maximum (FWHM) of the fat-referenced muscle fat infiltration (MFI) in the left anterior thigh. The histogram over all voxels in the region of interest is plotted both for 5° (blue line) and 10° (orange line), respectively. The FWHM for this subject is marked by the horizontal lines for each flip angle, respectively. The participant closest to the mean age and body mass index (BMI) (56-year-old participant with BMI of 27.5 kg/m²) was chosen

TABLE 3 Paired t-tests comparing 5° against 10° at the full width at half maximum (FWHM) in histogram over the fat-referenced muscle fat infiltration estimate in each voxel for each muscle region of interest

Measurand	t	p value	95% confidence interval (% units)
Left rectus femoris	5.89	<0.0001	0.6-1.23
Right rectus femoris	0.93	0.36	-0.23-0.62
Pooled rectus femoris	3.48	0.001	0.23-0.88
Left anterior thigh	4.89	<0.0001	0.28-0.67
Right anterior thigh	3.09	0.003	0.09-0.45
Pooled anterior thigh	5.24	<0.0001	0.23-0.52
Left posterior thigh	0.56	0.58	-0.25-0.14
Right posterior thigh	-0.93	0.35	-0.25-0.09
Pooled posterior thigh	-1.02	0.31	-0.20-0.07
Total thigh	2.65	0.01	0.04-0.27

Also presented are *p* values and 95% confidence intervals (in percentage units) for each of the 10 muscle regions. Significant differences (*p* < 0.05) in the FWHM measurements are shown in bold.

A quantitative MFI estimate invariant to T1 bias is crucial in multicenter, multimodality and longitudinal acquisitions because slight changes in parameter settings could affect TR and the actual flip angle and hence also the T1 weighting of the images.

The histogram analysis, illustrated in Figure 7, indicates that there was higher SNR in the 10° flip angle data compared with 5°, even if the differences were not visually observable in the images (Figure 1). The MFI measurements were, however, not only dependent on noise, but also on anatomical variations in the region of interest. This was evident in Table 3 by the significant differences when investigating the middle slice of the posterior thigh compared with no significant differences when looking at the whole muscle. The effect of anatomical variation needs to be taken into consideration when analyzing longitudinal MFI changes. Because the anatomical variation in muscles/muscle groups can overpower the variance from signal noise, it is crucial that the same area of interest is analyzed between the measurements. Therefore, methods including whole muscle coverage are preferable.

Despite the significantly different noise characteristics between the two flip angles there were no statistically significant differences in terms of repeatability. This indicates that it is not solely SNR that affects repeatability. Other potential factors that could affect the repeatability are eddy current effects and B1-inhomogeneities. Both these effects tend to increase with increased field strength and/or stronger gradients. In this study, we corrected for eddy current effects caused by the bipolar gradient readout. Also, fat-referenced MFI has been shown to be insensitive to B1 inhomogeneities.³⁰ Looking at Figure 6, we can see a slightly different pattern of the F-ratio between fat-referenced and FF methods, where

there is a tendency towards higher variance at 5° for the fat-referenced method and vice versa for the FF method. The reason for this might be that the increase in SNR using a 10° flip angle gives a slightly lower variance. However, for the FF technique, the increase in T1 bias affects the absolute variance and the influence of increased SNR is not seen.

In a study by Kühn et al., the maximum SNR was achieved at a flip angle of 10°. ¹⁸ Different parameters influence the SNR. However, theoretical calculations estimated the maximal signal to be achieved at 10.7° for fat signal and at 6.9° for muscle signal for a spoiled gradient echo sequence using previously reported T1 values for fat and water ³¹ and a TR equal to 6.69 ms (which was used in the current study). The 5° flip angle was chosen to decrease the SNR compared with 10° while maintaining high enough signal for sufficient whole-muscle coverage segmentation.

One limitation to the current study was that only two flip angles were used. This limitation was necessary to limit scan time, while still collecting representative data. The SNR is not linearly dependent on the flip angle and the effect of choosing the higher flip angles of 10° and 5° compared with lower flip angles of 2° and 3° would also have been valuable to assess. Another limitation was that the data were collected using a protocol that was optimized to give high SNR, in general using multiple echoes and dedicated surface coils at high field strength. A more rapid scan with lower SNR would possibly be even more affected by different flip angles.

To conclude, the current study showed that fat-referenced MFI was insensitive to T1 weighting and that the higher flip angle provided advantages in noise characteristics. For these reasons, it is suggested to acquire data at a 10° flip angle with whole-volume acquisition when measuring fat-referenced MFI.

ACKNOWLEDGEMENTS

Part of this work was funded by Vetenskapsrådet (the Swedish Research Council), Grant VR 2019-0475.

CONFLICT OF INTEREST

AP, ACSH and ST have no conflicts of interest to declare. TR, ODL, JW and MB receive salaries and are stockholders of AMRA Medical AB. AK is a stockholder of AMRA Medical AB. This does not alter our adherence to *NRM in Biomedicine's* policies on sharing data and material.

DATA AVAILABILITY STATEMENT

The data that support the findings of this study are available from the corresponding author upon reasonable request.

ORCID

Anette Karlsson  <https://orcid.org/0000-0003-0438-6951>

REFERENCES

1. Delmonico MJ, Harris TB, Visser M, et al. Longitudinal study of muscle strength, quality, and adipose tissue infiltration. *Am J Clin Nutr*. 2009;90(6):1579-1585.
2. Elliott J, Jull G, Noteboom JT, Darnell R, Galloway G, Gibbon WW. Fatty infiltration in the cervical extensor muscles in persistent whiplash-associated disorders: a magnetic resonance imaging analysis. *Spine*. 2006;31(22):E847-E855.
3. Gerdle B, Forsgren MF, Bengtsson A, et al. Decreased muscle concentrations of ATP and PCR in the quadriceps muscle of fibromyalgia patients--a 31P-MRS study. *Eur J Pain*. 2013;17(8):1205-1215.
4. Karlsson A, Leinhard OD, Aslund U, et al. An investigation of fat infiltration of the multifidus muscle in patients with severe neck symptoms associated with chronic whiplash-associated disorder. *J Orthop Sports Phys Ther*. 2016;46(10):886-893.
5. Zoico E, Rossi A, Di Francesco V, et al. Adipose tissue infiltration in skeletal muscle of healthy elderly men: relationships with body composition, insulin resistance, and inflammation at the systemic and tissue level. *J Gerontol A Biol Sci Med Sci*. 2010;65(3):295-299.
6. Bonati U, Hafner P, Schadelin S, et al. Quantitative muscle MRI: A powerful surrogate outcome measure in Duchenne muscular dystrophy. *Neuromuscul Disord*. 2015;25(9):679-685.
7. Willcocks RJ, Rooney WD, Triplett WT, et al. Multicenter prospective longitudinal study of magnetic resonance biomarkers in a large duchenne muscular dystrophy cohort. *Ann Neurol*. 2016;79(4):535-547.
8. Goodpaster BH, Stenger VA, Boada F, et al. Skeletal muscle lipid concentration quantified by magnetic resonance imaging. *Am J Clin Nutr*. 2004;79(5):748-754.
9. West J, Romu T, Thorell S, et al. Precision of MRI-based body composition measurements of postmenopausal women. *PLoS ONE*. 2018;13(2):e0192495.
10. Machann J, Bachmann OP, Brechtel K, et al. Lipid content in the musculature of the lower leg assessed by fat selective MRI: intra- and interindividual differences and correlation with anthropometric and metabolic data. *J Magn Reson Imaging*. 2003;17(3):350-357.
11. Yoshiko A, Hioki M, Kanehira N, et al. Three-dimensional comparison of intramuscular fat content between young and old adults. *BMC Med Imaging*. 2017;17(1):12-20.
12. Schick F, Machann J, Brechtel K, et al. MRI of muscular fat. *Magn Reson Med*. 2002;47(4):720-727.
13. Hamilton G, Yokoo T, Bydder M, et al. In vivo characterization of the liver fat (1)H MR spectrum. *NMR Biomed*. 2011;24(7):784-790.
14. Yu H, Shimakawa A, McKenzie CA, Brodsky E, Brittain JH, Reeder SB. Multiecho water-fat separation and simultaneous R2* estimation with multifrequency fat spectrum modeling. *Magn Reson Med*. 2008;60(5):1122-1134.

15. Dixon WT. Simple proton spectroscopic imaging. *Radiology*. 1984;153(1):189-194.
16. Reeder SB, Hu HH, Sirlin CB. Proton density fat-fraction: a standardized MR-based biomarker of tissue fat concentration. *J Magn Reson Imaging*. 2012;36(5):1011-1014.
17. Hong CW, Hamilton G, Hooker C, et al. Measurement of spleen fat on MRI-proton density fat fraction arises from reconstruction of noise. *Abdom Radiol*. 2019;44(10):3295-3303.
18. Kühn JP, Jahn C, Hernando D, et al. T1 bias in chemical shift-encoded liver fat-fraction: role of the flip angle. *J Magn Reson Imaging*. 2014;40(4):875-883.
19. Hu HH, Nayak KS. Quantification of absolute fat mass using an adipose tissue reference signal model. *J Magn Reson Imaging*. 2008;28(6):1483-1491.
20. Dahlqvist Leinhard O, Johansson A, Rydell J, et al. Quantitative Abdominal Fat Estimation using MRI. Proceedings - International Conference on Pattern Recognition (ICPR). 2008;4761764.
21. Romu T, Borga M, Dahlqvist Leinhard O. MANA - Multi scale adaptive normalized averaging. Proceedings - International Symposium on Biomedical Imaging (ISBI) 2011; art. no. 5872424:361-364.
22. Peterson P, Romu T, Brorson H, Dahlqvist Leinhard O, Mansson S. Fat quantification in skeletal muscle using multigradient-echo imaging: Comparison of fat and water references. *J Magn Reson Imaging*. 2016;43(1):203-212.
23. Berin E, Hammar ML, Lindblom H, Lindh-Astrand L, Spetz Holm AC. Resistance training for hot flushes in postmenopausal women: Randomized controlled trial protocol. *Maturitas*. 2016;85:96-103.
24. Romu T, Dahlstrom N, Leinhard OD, Borga M. Robust water fat separated dual-echo MRI by phase-sensitive reconstruction. *Magn Reson Med*. 2017;78(3):1208-1216.
25. Yu H, Shimakawa A, McKenzie CA, et al. Phase and amplitude correction for multi-echo water-fat separation with bipolar acquisitions. *J Magn Reson Imaging*. 2010;31(5):1264-1271.
26. Karlsson A, Rosander J, Romu T, et al. Automatic and quantitative assessment of regional muscle volume by multi-atlas segmentation using whole-body water-fat MRI. *J Magn Reson Imaging*. 2015;41(6):1558-1569.
27. Linge J, Borga M, West J, et al. Body composition profiling in the UK Biobank Imaging Study. *Obesity*. 2018;26(11):1785-1795.
28. Borga M, Ahlgren A, Romu T, Widholm P, Dahlqvist Leinhard O, West J. Reproducibility and repeatability of MRI-based body composition analysis. *Magn Reson Med*. 2020;84(6):3146-3156.
29. Bland JM, Altman DG. Measurement error. *BMJ*. 1996;313(7059):1654.
30. Andersson T, Romu T, Karlsson A, et al. Consistent intensity inhomogeneity correction in water-fat MRI. *J Magn Reson Imaging*. 2015;42(2):468-476.
31. Bazelaire CMJ, Duhamel GD, Rofsky NM, Alsop DC. MR imaging relaxation times of abdominal and pelvic tissues measured in vivo at 3.0 T: preliminary results. *Radiology*. 2004;230(3):652-659.

SUPPORTING INFORMATION

Additional supporting information may be found online in the Supporting Information section at the end of this article.

How to cite this article: Karlsson A, Peolsson A, Romu T, et al. The effect on precision and T1 bias comparing two flip angles when estimating muscle fat infiltration using fat-referenced chemical shift-encoded imaging. *NMR in Biomedicine*. 2021;e4581. <https://doi.org/10.1002/nbm.4581>